The Journal of Experimental Biology 216, 2974-2982

doi:10.1242/jeb.083667

RESEARCH ARTICLE

Power output of skinned skeletal muscle fibres from the cheetah (*Acinonyx jubatus*)

Timothy G. West[1], Christopher N. Toepfer[2], Roger C. Woledge[1], Nancy A. Curtin[1,2,*] Anthea Rowlerson[3], Michaeljohn Kalakoutis[3], Penny Hudson[1] and Alan M. Wilson[1]

[1]Structure and Motion Laboratory, The Royal Veterinary College, Hawkshead Lane, South Mymms AL9 7TA, UK, [2]Molecular Medicine Section, NHLI, SAF Building, Imperial College London, London SW7 2AZ, UK and [3]Centre for Human & Aerospace Physiological Sciences, Shepherd's House, Guy's Campus, Kings College London, London SE1 1UL, UK

*Author for correspondence (n.curtin@imperial.ac.uk)

SUMMARY

Muscle samples were taken from the gluteus, semitendinosus and longissimus muscles of a captive cheetah immediately after euthanasia. Fibres were 'skinned' to remove all membranes, leaving the contractile filament array intact and functional. Segments of skinned fibres from these cheetah muscles and from rabbit psoas muscle were activated at 20°C by a temperature-jump protocol. Step and ramp length changes were imposed after active stress had developed. The stiffness of the non-contractile ends of the fibres (series elastic component) was measured at two different stress values in each fibre; stiffness was strongly dependent on stress. Using these stiffness values, the speed of shortening of the contractile component was evaluated, and hence the power it was producing. Fibres were analysed for myosin heavy chain content using gel electrophoresis, and identified as either slow (type I) or fast (type II). The power output of cheetah type II fibre segments was 92.5±4.3 W kg^{-1} (mean ± s.e., 14 fibres) during shortening at relative stress 0.15 (the stress during shortening/isometric stress). For rabbit psoas fibre segments (presumably type IIX) the corresponding value was significantly higher (P<0.001), 119.7±6.2 W kg^{-1} (mean ± s.e., 7 fibres). These values are our best estimates of the maximum power output under the conditions used here. Thus, the contractile filament power from cheetah was less than that of rabbit when maximally activated at 20°C, and does not account for the superior locomotor performance of the cheetah.

Key words: energetics, muscle mechanics, rabbit, contraction.

Received 6 December 2012; Accepted 2 April 2013

INTRODUCTION

The cheetah [*Acinonyx jubatus* (Schreber 1775)] is the fastest running animal with a top speed of 29 m s^{-1} (Sharp, 1997), considerably faster than racehorses (Spence et al., 2012) and racing greyhounds (Usherwood and Wilson, 2005), which can only achieve about 20 m s^{-1}. Cheetah hunting also involves extremely rapid acceleration and the power required for this acceleration has been measured in wild cheetahs (Wilson et al., 2013). Averaged across three gait cycles the power can be as high as 90 W kg^{-1} of body mass. About half of the cheetah's body mass is muscle, so this is equivalent to 180 W kg^{-1} of muscle. This is one of the highest recorded values for a terrestrial mammal and suggests that cheetah muscle may have unusually powerful characteristics that contribute to its high running speed and acceleration. It has already been reported (Hyatt et al., 2010; Goto et al., 2013) that the muscles of the cheetah contain a very high proportion of the fastest and most powerful mammalian muscle fibre types (Type IIB and IIX).

We had the opportunity to obtain post-mortem cheetah muscle fibres from a captive animal and have measured their power output while shortening under different loads. The aim was to investigate whether the maximum power was large compared with that of muscle from an animal that is less specialized for running speed; for this comparison, experiments were done on fast-twitch fibres from rabbit. Skinned muscle fibres were used for two reasons: their power output could be measured after the unavoidable delay between collecting cheetah samples and testing them, and skinned fibres allow comparison of power output of the contractile filaments themselves.

Cheetah and rabbit fibres contracted under identical conditions of activation, temperature and movement pattern. To activate the fibres we used the temperature-jump method (Bershitsky and Tsaturyan, 1989), which reliably produces repeated contractions at temperatures closer to *in vivo* temperature than those conventionally used with Ca^{2+} activation of skinned fibres. We found that under the conditions used here, notably 20°C and constant velocity shortening, the cheetah fast-twitch fibres did not produce higher power than rabbit fast-twitch fibres. The results suggest that either the superior locomotor performance of the cheetah is due to factors other than the contractile filament function itself, or that if there is a difference in contractile filament power output *in vivo*, the difference does not exist under the conditions used here. More *in vivo*-like conditions that could be explored include higher temperature, submaximal activation, and/or a more life-like pattern of movement.

MATERIALS AND METHODS

Muscle fibre preparation and storage

A captive cheetah (male, age 6.5 years, mass 41 kg), with probable renal failure, was euthanized at the Royal Veterinary College with an overdose of barbiturates. It was a mature, but not aged animal. Bundles of skeletal muscle fibres (10 mm in diameter, 40–50 mm long) were dissected from the gluteus medius, semitendinosus and

longissimus muscles. Functionally, gluteus medius is a hip extensor, semitendinosus is a hip extensor and knee flexor (Hudson et al., 2011) and longissimus extends the spine. Fibres were also obtained from the psoas muscles of two female New Zealand White rabbits as previously described (He et al., 1999).

The cheetah became available unexpectedly, so experiments were done on skinned muscle fibres because they can be stored for later study. Intact mammalian fibres must be used within hours of removal from the animal, which was not possible on this occasion. Fibre bundles were permeabilized at 4°C in a skinning solution (Table 1) containing increasing concentrations of glycerol, as described previously (Thirlwell et al., 1994; He et al., 1997; He et al., 1998). The permeabilized fibre bundles were stored at −20°C in skinning solution made up in 50% glycerol and were used within 8 weeks. Single muscle fibre segments were dissected away from the fibre bundle in a relaxing solution (Table 1) containing 0.5% Triton X-100 at 7°C on a temperature-controlled stage of a dissecting microscope. Aluminium foil 'T-clips' (Photofabrication, St Neots, UK) were placed on the ends of the fibre segment (length between 0.8 and 1.5 mm). The clips were attached with shellac to stainless steel wire hooks, one connected to a force transducer (AE801; HJK Sensoren + Systeme, Friedberg, Germany) and the other to a purpose-built motor as described elsewhere (Bershitsky et al., 1996). The fibre segment was suspended in 30 µl of relaxing solution in the quartz trough of an aluminium temperature-controlled microscope stage.

Fibre dimensions and units

While in relaxing solution, the sarcomere length (SL) was set to 2.4 µm using laser diffraction; the filament lengths in mammalian muscle are such that this SL is optimal for force development. The segment length at a SL of 2.4 µm was our reference length (L_o). Fibre segment length, width and depth were measured using a Zeiss (Jena, Germany) ACM microscope with ×40 water-immersion objective. Cross-sectional area (CSA) was calculated from the measured width and depth, assuming an elliptical cross-section; no correction was made for possible swelling as a result of skinning.

The values of L_o and CSA were used to take account of variations in the size of the fibre segments. Density was assumed to be 1 kg dm^{-3} when converting from muscle fibre volume to mass. Force is reported either as stress (=force/CSA, units kPa) or in some contexts as relative stress (stress during shortening/isometric stress produced before shortening in the same contraction, F_s/F_i). Velocity of shortening is reported in relative units: change in length $(\Delta L)/L_o$ s^{-1}. Stiffness (=stress change/relative length change) is reported in units of MPa.

Power is reported in units of W kg^{-1} muscle. Relative power values were multiplied by isometric stress (kPa) to give power in units of W kg^{-1}, assuming 1 dm^3 corresponds to 1 kg.

$$\text{Power} = \frac{F_s}{F_i} \times \frac{\Delta L}{L_o} \times \frac{1}{\Delta t} \times F_i \,, \quad (1)$$

$$\text{Units for power} = \frac{\text{kPa}}{\text{kPa}} \times \frac{\text{m}}{\text{m}} \times \frac{1}{\text{s}} \times \text{kPa} = \frac{\text{W}}{\text{kg}} \,. \quad (2)$$

Fibre activation

Fibre segments were activated by the temperature-jump (T-jump) method (Bershitsky and Tsaturyan, 1989). The principle of the method is that at low temperature, the active fibre segment produces little force because few cross-bridges are attached and many of these produce low force. At the higher temperature, the active fibre segment gives more force both because more cross-bridges are attached and because more of them produce a high force.

The T-jump apparatus, based on the design by Linari et al. (Linari et al., 1998), consisted of two temperature-controlled stages that were moved horizontally by a stepper motor. The low temperature was ~2°C (range 1.6–2.1°C) and the high temperature was 20°C. Each stage carried a quartz platform on which were placed two separate drops (30 µl) of solution. The stages were moved so that the fibre segment was immersed successively in the following solutions: (1) pre-activating at low temperature for 2 min, (2) activating at low temperature, (3) activating at high temperature and finally (4) relaxing at high temperature (see Fig. 1A).

LabView software was used to control the stage position and fibre segment length, and recorded the digitized output signals from the force transducer and motor at 1 or 10 kHz.

Protocol for measuring power output by the contractile component

The fibre segments were activated by increasing [Ca^{2+}] at low temperature; temperature was then rapidly increased (T-jump) and

Table 1. Constituents of the solutions

Component	Skinning solution	Relaxing solution	Pre-activating solution	Activating solution
TES	0	100	100	100
Imidazole	6	0	0	0
Magnesium acetate	8	0	0	0
Magnesium chloride	0	7.8	6.8	6.5
Potassium propionate	70	0	0	0
ATP	7	5.7	5.7	5.7
EGTA	5	25	0.1	0
Calcium EGTA ([Ca^{2+}]=32 µmol l^{-1})	0	0	0	25
HDTA	0	0	24.9	0
Creatine phosphate	0	21.2	21.2	21.2
Glutathione	0	20	20	20
PMSF	10	0	0	0
Leupeptin	4	0	0	0
Trypsin inhibitor	50	0	0	0

All concentrations are in units of mmol l^{-1}, except leupeptin and trypsin inhibitor which are in mg l^{-1}.

Skinning solutions were made up with 12.5, 25 and 50% glycerol for the permeabilization process; permeabilized fibres were stored in 50% glycerol skinning solution. Solution pH was 7.1 at 20°C.

TES, *N*[Tris(hydroxy-methyl)methyl]-2-aminoethanesulfonic acid; ATP, adenosine 5′-triphosphate disodium salt hydrate; EGTA, ethylene glycol-bis(2-aminoethylether)-*N,N,N′,N′*-tetraacetic acid; HDTA, 1,6-diaminohexane-*N,N,N′,N′*,-tetraacetic acid; PMSF, phenylmethanesulphonyl fluoride.

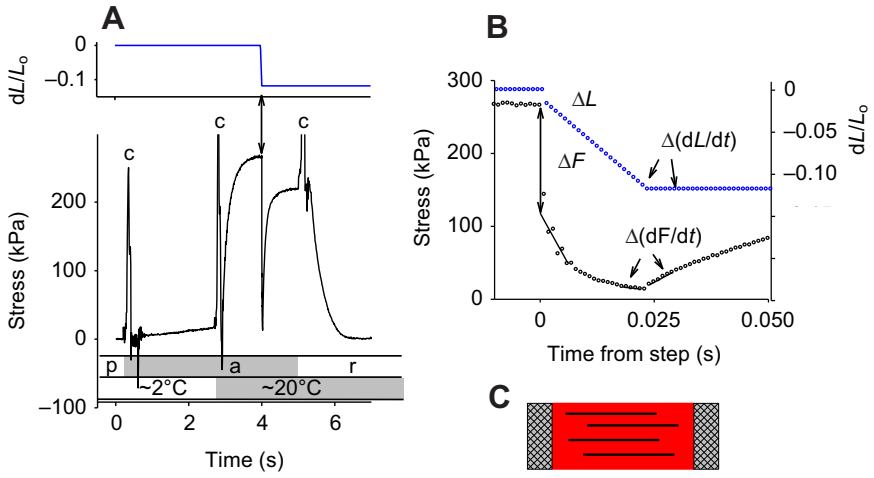

Fig. 1. (A) Diagram showing contraction protocol. Upper panel shows the imposed length changes (L, length; L_o, reference length); lower panel shows the record of stress, with solutions (p, pre-activating solution; a, activating solution; r, relaxing solution) and temperature indicated below. The arrow indicates the time of the length step and ramp shortening. The spikes labelled c indicate artefacts that occurred during solution change. (B) Expanded section of the stress (F) and length (L) records giving an overview of the measurements used to get S_1, the series elastic component (SEC) stiffness during the step $\Delta F/\Delta L$, and S_2, the SEC stiffness at the end of the ramp, $\Delta(dF/dt)/\Delta(dL/dt)$. Stress changes are shown in more detail in Fig. 2. (C) Diagram of a segment of a skinned fibre. The contractile part is red, the non-contractile ends are grey.

when isometric stress had been developed the fibre length was decreased in a 'step and ramp' pattern (Fig. 1B). Each fibre segment performed a series of contractions with different ramp velocities and different step sizes.

Our aim was to measure the power produced by the contractile component (CC), which is the product of stress and the velocity of CC shortening. In the next section we will describe how we analysed the records to obtain the CC power, which involves separating the total shortening of the fibre segment into that due to the CC and that due to the non-contractile component(s) using methods previously described (Sonnenblick, 1964; Curtin et al., 1998; Mellors and Barclay, 2001). The stiffness of the non-contractile components will be evaluated as part of the analysis; Fig. 1B and Fig. 2 show, respectively, an overview and an example record. It should be noted that this stiffness is, to a large extent that of the damaged ends of the skinned fibre segment (Fig. 1C); in contrast, *in vivo* and in isolated, intact muscle fibres the non-contractile stiffness is dominated by the tendons. The mechanical properties of these damaged ends were found to be different from those of the tendons of muscle *in vivo* and of isolated, intact muscle fibres. In particular, the stiffness of the skinned fibre series elastic component(s) (SEC) (damaged ends) varied with stress, whereas the stiffness of the tendon was independent of stress except at very low stress.

In the following description SEC refers to the non-contractile parts of the skinned fibre segment. The principles underlying separation of SEC and CC shortening are (1) the stress in SEC and CC is the same and equal to the observed stress, in other words they are mechanically in series, (2) the total length change is the sum of the SEC length change and the CC length change, and (3) the length of the SEC depends solely on stress (and not on velocity of movement). Thus, the method assumes that the SEC can change its length much more quickly than the CC. For this reason the SEC stiffness can be measured when there is a sudden alteration in rate of length change.

The dependence of SEC stiffness on stress could be evaluated using the two parts of each record where there as an abrupt change; that is, at the step and at the end of the ramp. Two values of the

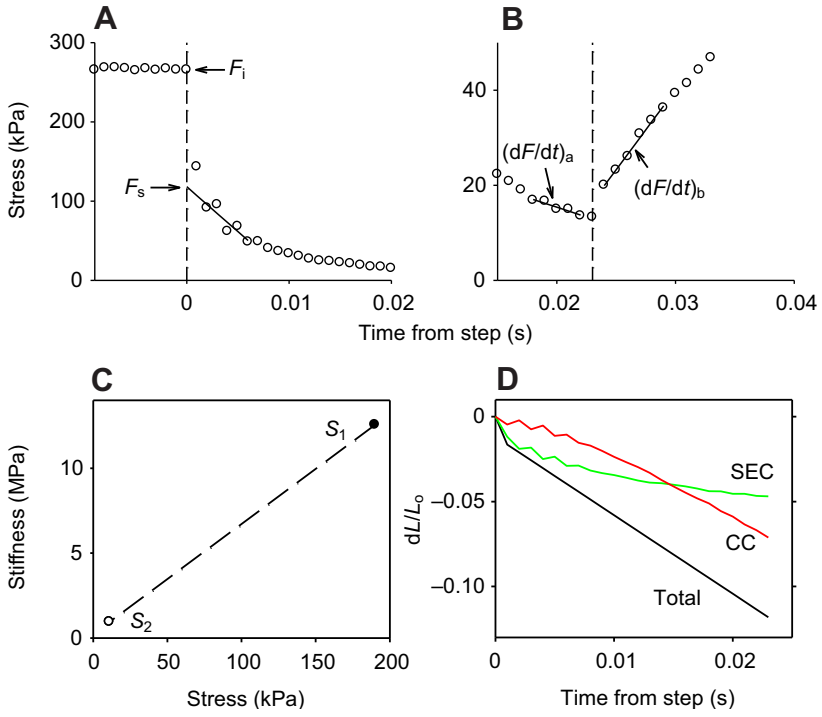

Fig. 2. (A) Expanded section of the stress around the step. The vertical dashed line marks the time of the step. F_i, isometric stress before the step; F_s, stress value at end of the step found by extrapolation; $\Delta F=F_i-F_s$. (B) Expanded section of the stress around the end of the ramp. The vertical dashed line marks the end of the ramp. $(dF/dt)_a$ is the rate of stress change at the end of the ramp, and $(dF/dt)_b$ is the rate of stress change after the end of the ramp. $\Delta(dF/dt)$=absolute value of $[(dF/dt)_a-(dF/dt)_b]$. (C) The relationship between stress and SEC stiffness measured at the step (S_1) and at the end of ramp shortening (S_2) in the record shown in A and B, respectively. S_1 is plotted against the average of F_i and F_s. The gradient of the dashed line, 0.0648 MPa kPa^{-1}, describes the variation in SEC stiffness with stress. (D) The time course of total length change of the fibre segment (black) and also the change in length of the SEC (green) and of the contractile component (CC, red) calculated using the stress and the SEC stiffness as described in Materials and methods.

SEC stiffness were measured in each record (Fig. 2A,B), and the corresponding relationship between stiffness and stress is shown in Fig. 2C. From this relationship the SEC stiffness at any stress (and thus at any time during the record) can be read off the graph. At each time point during the ramp shortening, the rate of SEC shortening was $(dF/dt)/S_F$, where dF/dt is the rate of change of stress and S_F is the stiffness at stress=F.

The time course of SEC length change is found by integration and is shown in Fig. 2D.

The shortening of the CC is found by subtracting the SEC shortening from the total shortening. Power produced by the CC was evaluated as the product of relative force (or stress) and the rate of change of the CC.

Successful mechanical experiments were done on 18 cheetah and seven rabbit fibre segments; of the cheetah fibres, 15 were typed as slow or fast twitch on the basis of gel electrophoresis as described below.

Curve fitting to evaluate peak power

Peak power was evaluated by considering two functions fitted to the observed values of power *versus* relative stress. (1) Regression lines for the relationship between power and relative stress (F_s/F_i) were calculated by a robust method (MatLab 'robustfit') that minimizes the influence of outlying points as described by Holland and Welsch (Holland and Welsch, 1977). The regression gave values for the mean power across the range of stress values investigated and also gave an intercept on the relative stress axis (F^*/F_i). (2) The observed power was also compared with the following function, describing the relationship between stress during shortening and power (W kg^{-1}), which is based on Hill's hyperbolic force–velocity relationship as modified by Edman et al. (Edman et al., 1976):

$$\text{Power} = F_s \times V_{max} \times \left(1 - \frac{F_s/F_i}{F^*/F_i}\right) \Big/ \left(1 + G \times \frac{F_s/F_i}{F^*/F_i}\right), \quad (3)$$

where F_s is the stress during shortening (kPa), F_i is the isometric stress (kPa) and F^*/F_i is the intercept of the regression analysis described above, V_{max} is the maximum shortening velocity ($dL/L_o\,s^{-1}$), and G is a constant. This function, assuming differing values of V_{max} and G, neither of which could be determined in the experiments reported here, was compared with the experimental results.

Fibre typing

Fibre segments 1–3 mm in length from cheetah muscles were dissolved in 20 µl of sample buffer (Laemmli, 1970) and heated at 100°C for 3 min. Samples (4 µl) were loaded into 0.75 mm thick gels in a Hoefer 'mighty small' apparatus. Two different stacking–separating gel combinations were used, a 4.5% stacking gel with a 7.5% separating gel containing 30% glycerol (Picquet and Falempin, 2003) and a 4% stacking gel with a 9% separating gel both containing 30% glycerol (Blough et al., 1996). The gels were run following a previous method (Picquet and Falempin, 2003) with minor modifications. Over a 12 h period, a constant voltage of 100 V was set until the Bromophenyl Blue marker had migrated significantly (~2 cm) into the separating gel, at which point the voltage was increased to 180 V for the remainder of the run. Gels were subsequently silver stained (Morrissey, 1981) to reveal the myosin heavy chain bands. A sample of gluteus muscle, which contains both slow- and fast-twitch fibres, was treated as for the fibre segments and used as a standard. Two clearly separated bands were seen in this standard, which we assume to be from the fast- and slow-twitch fibres. We did not see any convincing subdivisions of the fast band and thus were not able to identify the two types of fast-twitch fibres that these muscles of the cheetah are known to contain (Goto et al., 2013).

RESULTS

Of the 15 cheetah fibre segments analysed by gel electrophoresis, four were identified as slow-twitch and 11 as fast-twitch fibres. As will be described below, the power output from the fibre segments identified as slow twitch on the gels was considerably less than that of those identified as fast twitch. The three segments for which there are no gel data were assumed to be fast twitch because their mechanical performance matched that of the fibre segments identified as fast twitch.

Analysis of all the individual mechanical records, like the example shown in Fig. 1B and Fig. 2, indicated that SEC stiffness, which is probably due to the non-contractile material at the ends of the fibre segments, was proportional to stress during a contraction. This rather unexpected variation of stiffness with stress was not unique to this example record. The same dependence was seen when results from different contractions and from different fibre segments were pooled (Fig. 3).

As described in Materials and methods, we used the stiffness of the SEC (non-contractile parts of the skinned fibre segment) to evaluate the velocity of shortening of the CC. The relationship between stress and the velocity of CC shortening is shown for cheetah fast- and slow-twitch fibre segments and for rabbit fibre segments in Fig. 4. As expected, the slow-twitch cheetah fibre velocities (Fig. 4C) are well below those for the fast-twitch fibres (Fig. 4A). For both cheetah and rabbit the relative stress–velocity results for the fast-twitch fibres fall along the expected hyperbolic relationship. Cheetah fibres from different anatomical sites (shown by different colours in the figure) behaved similarly. It is clear that the range of velocities we used was not sufficient to cover the entire stress–velocity curve and we were unable to evaluate the maximum

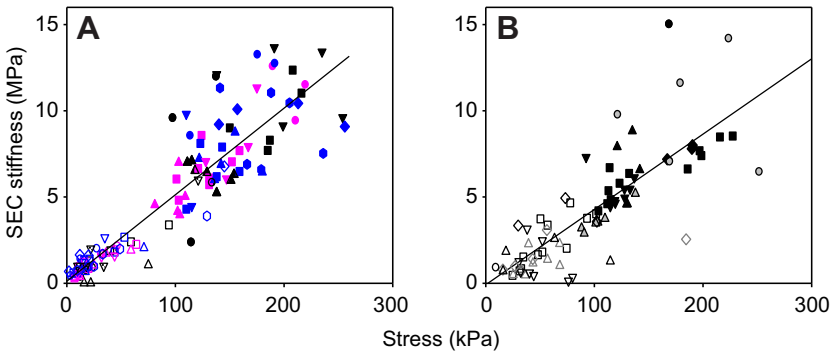

Fig. 3. The relationship between the SEC stiffness and stress during step shortening (filled symbols) and at the end of ramp shortening (open symbols). (A) Pairs of SEC stiffness values from 70 contractions of cheetah fibre segments measured by the method described in Materials and methods. Results for four fibre segments from gluteus, black; four from semitendinosus, pink; and six from longissimus, blue. Between one and eight contractions per fibre. Different symbols indicate results for different fibre segments. Regression line: y=0.0502x+0.1156, r^2=0.8329. (B) Pairs of SEC stiffness values from 41 contractions of seven fibre segments (different symbols) from psoas muscle of rabbit. Between one and 12 contractions per fibre segment. Regression line: y=0.0431x–0.0852, r^2=0.6528.

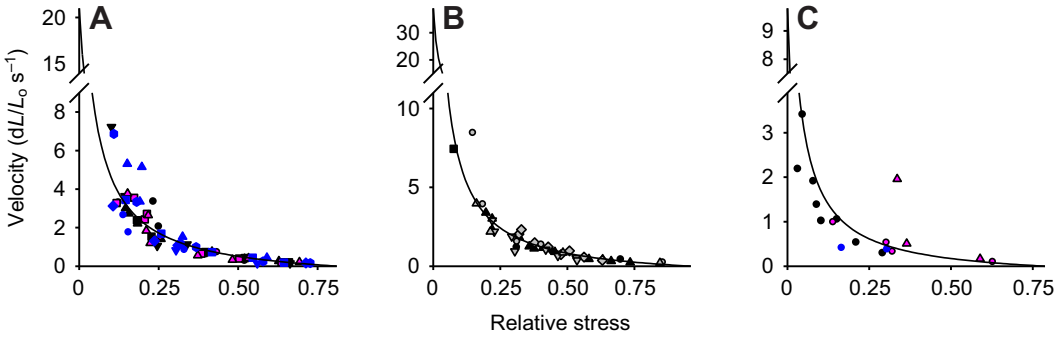

Fig. 4. Velocity–relative stress relationships. Relative stress is the average produced during the first part of ramp shortening, F_s, expressed relative to the isometric stress just before shortening, F_i. (A) Cheetah fast-twitch fibres: gluteus, black; semitendinosus, pink; longissimus, blue. F_s from first 33% of shortening. (B) Rabbit fast-twitch fibres from psoas. F_s from first 50% of shortening. (C) Cheetah slow-twitch fibres: gluteus, black; semitendinosus, pink; longissimus, blue. F_s from first 50% of shortening. Different symbols indicate results for different fibres. Lines are hyperbolic Hill relationships:

$$\text{Velocity} = V_{max} \times \frac{\left(1 - \frac{F_s/F_i}{F^*/F_i}\right)}{\left(1 + G \times \frac{F_s/F_i}{F^*/F_i}\right)},$$

where V_{max} is the maximum shortening velocity ($dL/L_o\ s^{-1}$), F^* is the relative stress intercept and G is a constant. The constants shown in Table 4 were fitted as described in the Discussion.

velocity of shortening (V_{max}). For an explanation of the lines in Fig. 4, see Discussion. See also Table 4.

The relationship between power output and relative stress as measured in individual records is shown in Fig. 5. Linear regression analysis was done in each case using a robust method (see Materials and methods) that reduces the influence of outlying points. The residuals about the fitted lines are also shown for each case and their distributions indicate that these regression lines are a reasonable summary of the results. The 95% population confidence intervals derived from the regression analysis are also shown. Eqn 3, which is based on the usual hyperbolic stress *versus* velocity relationship, did not fit the data better than the linear regression line, as judged either by the correlation coefficient or by the distribution of the residuals (not shown). In the Discussion we will return to the problem of estimating the peak power from the results shown in Fig. 5.

The isometric stress values and power at relative stress of 0.15 from the regression analysis for the different fibre types are summarized in Table 2. Within the range of relative stresses that were tested, the power decreases as relative stress increases. The slopes of the regression lines for the fast-twitch fibres from cheetah and rabbit are not significantly different, whereas the intercepts are (Table 3). Thus, the line for the cheetah fast-twitch fibres lies below that for the rabbit results. The power for the slow-twitch cheetah fibres is only about 20% that of fast-twitch fibres at all relative stress values.

DISCUSSION

Estimate of peak power output for skinned fibres

We were unable to obtain satisfactory measurements of power when the relative stress was below 0.1. Power is zero when stress is zero and, as stress increases, power rises to a peak and then falls at higher stresses. The linear regression (Fig. 5) thus cannot give a complete description of power output. The regression analysis gives values for the maximum observed power within the range of stresses that we tested (Table 2). These estimates of the maximum power may be less than, but cannot be greater than, the true peak power. Eqn 3, which is based on a hyperbolic force *versus* velocity relationship, is useful here because it provides a function that passes through the origin and has a defined peak power. This equation was used to

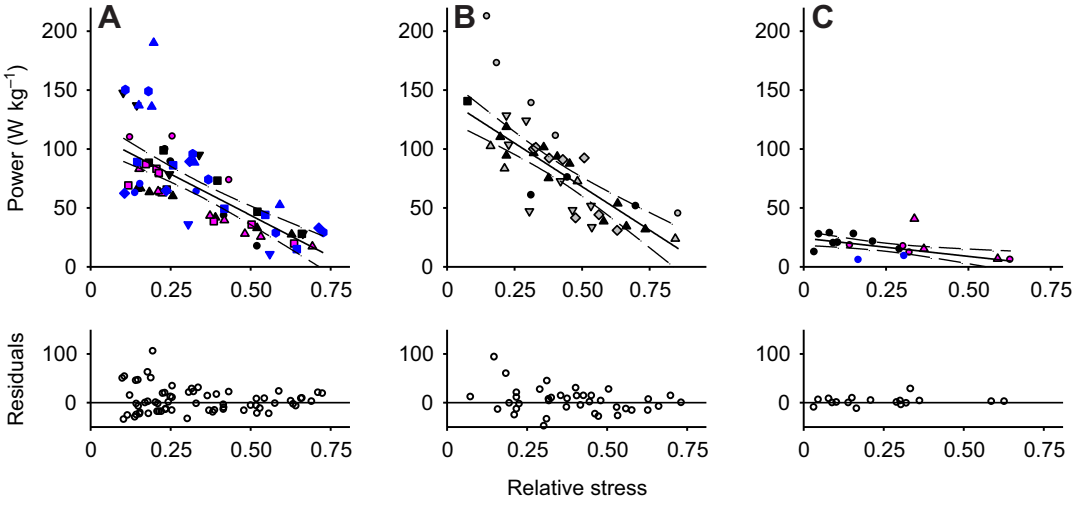

Fig. 5. Power–relative stress relationships. Power=relative stress × velocity × isometric stress for each record. Units $W\,kg^{-1}$=(kPa/kPa)×(m/m)×(1/s)×kPa, assuming 1 dm^3=1 kg. The relative stress and velocity values are shown in Fig. 4. (A) Cheetah fast-twitch fibres. (B) Rabbit fibres. (C) Cheetah slow-twitch fibres. Symbols as in Fig. 4. Solid line is the regression line and dashed lines are the 95% confidence intervals (see Results and Table 3). The residuals are shown in the lower set of graphs.

Table 2. Mechanical properties of skinned fibres from cheetah and rabbit

	Mean	*N*
Isometric stress (kPa)		
Cheetah (type I)	132.4±32.7	3
Cheetah (type II)	195.0±12.2	14
Rabbit (type IIX)	194.5±14.9	7
Maximum power (W kg^{-1})		
Cheetah (type I)	19.7±1.9	
Cheetah (type II)	92.5±4.3	**
Rabbit (type IIX)	119.7±6.2	

Isometric stress values are means ± s.e.m.; maximum power values are means ± s.e.
**Maximum power rabbit>cheetah, P<0.001.

explore the range of power curves that lie within the confidence intervals of the linear regression analysis and are thus compatible with our observations.

To assess how much our estimated maximum power falls short of the true peak power, we have considered for each of the muscle types, cheetah fast and slow twitch and rabbit fast twitch, a range of power *versus* stress curves that are compatible with the observations. As can be seen from Eqn 3, power is determined by the values of constants V_{max}, G and F*. The value of F* was taken to be equal to the intercept of the regression line on an x-axis (see Fig. 5). The range of values of G and V_{max} that give curves that fit within the confidence intervals of the regression was identified, subject to the constraint that V_{max} was less than $70L_o$ s^{-1} for fast-twitch fibres and $20L_o$ s^{-1} for slow-twitch fibres. The peak powers calculated from Eqn 3 using these G and V_{max} values fall within the small cyan area shown in each panel of Fig. 6. The maximum power from the regression line (red circle in Fig. 6) is close to this area, showing that our best estimates of peak power are unlikely to be much less than the actual peak power. The dashed blue line for each muscle type is an example of the complete power *versus* stress curve for the lowest V_{max} value that is compatible with the data. We show in Fig. 4 the stress *versus* velocity curves calculated using the lowest V_{max} and its corresponding G value, which are given in Table 4.

Comparison of rabbit and cheetah muscle

The results reported here do not show that cheetah muscle is more powerful than rabbit muscle, as would reasonably be expected from their locomotor performance. In fact, our best estimate of cheetah muscle power is significantly less than that of rabbit muscle (P<0.001, Table 2). We will discuss three factors (fibre types, temperature, and skinned *versus* intact fibres) that affect power and are likely to mean that *in vivo* power is higher than that observed here. These factors have not been fully explored for muscle from cheetah and rabbit; if they were, it might emerge that cheetah muscle is more powerful than rabbit muscle under conditions close to those *in vivo*. Alternatively, it could be that the muscles' capacity to produce power is very similar in these two species, and that the cheetahs' superior locomotor performance depends on other aspects of their design.

Fibre types

The rabbit fibres we used were most likely the fast IIX (=IID) type which makes up the majority of the psoas muscle (Hamalainen and Pette, 1993; Ducomps et al., 2004). The cheetah muscles we used contain both IIA and IIX fibres (Goto et al., 2013). We were unable to distinguish between these two fast fibre types by gel electrophoresis; the group of fibres used was probably a mixture of the two types. Thus, the power output of cheetah IIX fibres is likely to be greater than the value we report, which is probably from a mixed group of IIA and IIX fibres. We speculate that the power output of cheetah IIX fibres is greater than that of rabbit fibres of the same type. Confirmation of this point will need immuno-staining techniques to identify the fibre types, combined with measurements of their power output.

Temperature

Most previously published measurements of the power output of skinned mammalian muscle fibres have been made at temperatures below 20°C. A summary of these values, and the values reported here, is shown in Fig. 7A. Power output is known to be very temperature sensitive (Ranatunga, 1984; Ranatunga, 1998; Ranatunga, 2010), so it is not surprising that most of the earlier measurements are well below the value of about 100 W kg^{-1} at 20°C that we have found for both rabbit and cheetah fibres. The only published value for skinned fibres at a temperature higher than 20°C is for rat fibres at 30°C, which produced power of 166 W kg^{-1} (Knuth et al., 2006).

For intact rat and mouse muscle fibres, there are published values of power output covering a wide temperature range (Fig. 7B). It can be seen that the temperature dependence of power

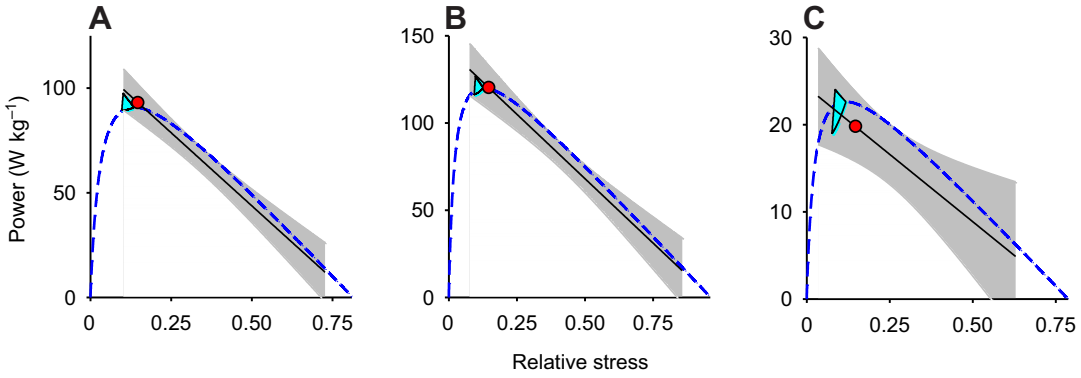

Fig. 6. Power–relative stress relationships. The solid black lines are the linear regression lines and grey areas show the 95% confidence intervals (see Fig. 5). The red filled circles on the regression lines show the power at relative stress 0.15. The dashed blue lines show power calculated from Eqn 3, which is based on the hyperbolic Hill relationship, using the constants shown in Table 4. The cyan area encloses the peak power values calculated using the velocity given by the hyperbolic Hill relationship (Eqn 3) subject to the following constraints: V_{max}<$70L_o$ s^{-1} for fast-twitch fibres and <20 L_o s^{-1} for slow-twitch fibres, and power within the 95% confidence intervals of the regression line.

Table 3. Linear regression of power (W kg^{-1}) on relative stress for skinned fibres from cheetah and rabbit

	Slope	Intercept	r^2	N
Cheetah (type I)	–30.9±9.7	24.3±2.9	0.384	17
Cheetah (type II)	–139.7±16.5	113.5±6.4	0.728	66
Rabbit (type IIX)	–147.7±19.2	141.9±8.7	0.775	41

Power=(slope×relative stress)+intercept. Slope and intercept are given ± s.e.

Table 4. Hill equation parameters for skinned fibres from cheetah and rabbit

	F^*	G	V_{max} (dL/L_o s^{-1})
Cheetah (type I)	0.787	31.3	9.86
Cheetah (type II)	0.813	24.3	21.1
Rabbit (type IIX)	0.961	42.4	39.4

F^*, relative stress intercept; G, constant; V_{max}, maximum shortening velocity. For details, see Discussion.

is steeper at temperatures below 20°C than at higher temperatures. This can be illustrated by drawing two straight lines through the rat data points; for the lower temperature range the slope is 5 (i.e. it corresponds to a Q_{10}=5) and for higher temperatures the slope is 2.25. To make a comparison of our skinned fibre results with other published values, we have assumed that these Q_{10} values also apply to the skinned fibres. The solid line in Fig. 7A has the same slopes as in Fig. 7B, but has been shifted vertically to pass through our measured power values for rabbit and cheetah. The line passes close to the values at 12°C previously reported for rabbit and for large felids. However, a substantial number of the previously reported power values lie below this line, including all the values reported for human muscle, and in particular the one value for human muscle at 20°C. This difference suggests that cheetah and rabbit muscles are inherently more powerful than human muscle, in agreement with the conclusion of Kohn and Noakes (Kohn and Noakes, 2013), and have a higher glycolytic capacity (Williams et al., 1997).

Comparison of skinned and intact fibres

It has previously been reported that the power output of skinned muscle fibres is less than that of intact muscle fibres of the same species at the same temperature. For example, Curtin and Woledge (Curtin and Woledge, 1988) found that intact fibres gave a maximum power output 65% greater than that of skinned fibres reported by Bone and colleagues (Bone et al., 1986); both studies used white muscle fibres of the dogfish at 12°C. A similar comparison of skinned and intact fibres has been made for frog. Ferenczi and colleagues (Ferenczi et al., 1984) reported experiments on skinned frog fibres showing that the curvature of the force *versus* velocity relationship was greater than literature values for intact muscle fibres also from frog (Edman et al., 1976; Edman and Hwang, 1977; Cecchi et al., 1978). A more curved force *versus* velocity relationship would mean a lower maximum power output if F^* (intercept on the force axis) and V_{max} (the maximum velocity of shortening) remained unchanged. Ferenczi and colleagues (Ferenczi et al., 1984) report that neither the isometric force nor the V_{max} values were significantly different between their skinned fibre and these intact fibre studies. Maximum power was, therefore, less in the skinned than in the intact fibres. We calculate from the parameters of the force *versus* velocity relationships given in these publications that the intact fibres produced on average 45% more power than the skinned fibres used by Ferenczi and colleagues (Ferenczi et al., 1984).

A similar difference can be seen in Fig. 7B where the measured power outputs for intact rat fibres is greater than that of skinned rat fibres, by 76% at 15°C and by 31% at 30°C. Would the same difference be found for the muscle from the species investigated here? As discussed above, we do not have enough observations at low force to establish the full force *versus* velocity range for the cheetah and rabbit skinned fibres. However, we did find the G values that gave peak powers compatible with our observations (Table 4). The G values are high, between 24 and 42, indicating that force *versus* velocity relationships are very curved. In contrast, the corresponding values for intact fibres from rat and mouse are less than 4 for fast-twitch fibres and less than 7.5 for slow-twitch fibres (Ranatunga, 1982; Ranatunga, 1984; Barclay, 1996). Thus, it seems likely that the force *versus* velocity relationship for intact cheetah fibres would be less curved and the power output greater than for skinned fibres as has been found for frog, dogfish and rat muscle. Experiments with intact fibres from cheetah and rabbit are required

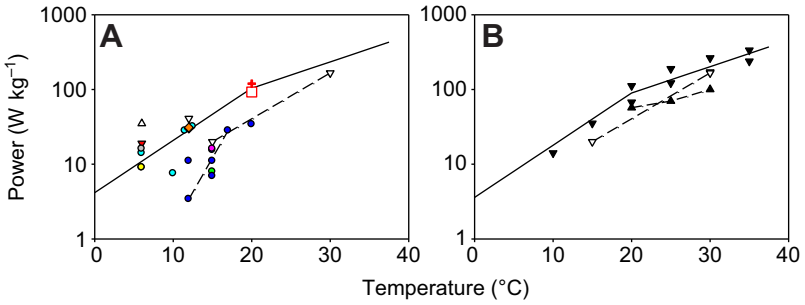

Fig. 7. Relationship between power output (log scale) of muscle from different mammalian species and temperature. (A) Skinned fibre results. Red square, cheetah (this report); red cross, rabbit (this report); white upward triangle, mouse (Seow and Ford, 1991); white downward triangle, rat (Bottinelli et al., 1991; Seow and Ford, 1991; Knuth et al., 2006); cyan circle, rabbit (Seow and Ford, 1991; He et al., 1999; Sun et al., 2001); green circle, goat (Hanes et al., 2008); yellow circle, sheep (Seow and Ford, 1991); orange diamond, lion and caracal (Kohn and Noakes, 2013); pink circle, horse (Rome et al., 1990); grey circle, cow (Seow and Ford, 1991); blue circle, human (Bottinelli et al., 1996; Widrick et al., 1996; He et al., 2000; Gilliver et al., 2009; Claflin et al., 2011; Kohn and Noakes, 2013). Dashed lines join values from the same study. Solid lines, which are drawn through the cheetah and rabbit results reported here, are calculated for Q_{10}=5.0 between 0 and 20°C, and Q_{10}=2.25 at temperatures >20°C. (B) Intact fibre results. Black upward triangle, mouse (Barclay et al., 2010); black downward triangle, rat (Ranatunga, 1998). Skinned fibre results. White downward triangle, rat (Knuth et al., 2006). Solid lines summarize the relationship for rat intact fibres; slopes as in A.

to test this conjecture and make a more complete comparison of these species.

Power output of cheetah muscles *in vivo*

Our best estimate of the average maximum power output by skinned cheetah muscle fibres of the fast-twitch type is 92.5 W kg^{-1}. How much power might be produced *in vivo*? At the *in vivo* temperature of 38°C, power would be increased to 400 W kg^{-1}, using a Q_{10} for power output of 2.25 as illustrated in Fig. 7. It is likely that intact fibres would produce about 50% more power than the skinned fibres used here: ~600 W kg^{-1}. This is an estimate of the power output of a mixed population of the two fast-twitch fibre types. The power output from the IIX fibre type would be higher, possibly approaching 1 kW kg^{-1}. Such large power outputs have previously been reported for two small land vertebrates: 0.95 kW kg^{-1} for lizard muscle at 39°C (Curtin et al., 2005) and 1.15 kW kg^{-1} from quail muscle *in vivo* (~40°C) (Askew et al., 2001). The similarity in the power output of the fibres from animals of such different sizes (40 kg cheetah, 5 g lizard and 40 g quail) agrees with the summary reported by Askew and colleagues (Askew et al., 2001) for flying animals ranging in size from bee to turkey based on *in vivo* measurements. In contrast, Seow and Ford (Seow and Ford, 1991) using skinned muscle fibres at low temperature (~5°C) found a strong negative correlation of power output with body mass across a range of mammalian species. Clearly, temperature and the type of preparation both have a big influence on the relationship between muscle power and body mass.

ACKNOWLEDGEMENTS

We thank Matthew Pead for helping us access the material.

AUTHOR CONTRIBUTIONS

The experiments were done by T.G.W., C.N.T., A.R., M.K., P.H. and A.M.W. The results were interpreted and the paper written by R.C.W., N.A.C. and A.R.

COMPETING INTERESTS

No competing interests declared.

FUNDING

This research was supported by the Biotechnology and Biological Sciences Research Council [grant no. BB/J018007/1].

REFERENCES

Askew, G. N., Marsh, R. L. and Ellington, C. P. (2001). The mechanical power output of the flight muscles of blue-breasted quail (*Coturnix chinensis*) during take-off. *J. Exp. Biol.* **204**, 3601-3619.

Barclay, C. J. (1996). Mechanical efficiency and fatigue of fast and slow muscles of the mouse. *J. Physiol.* **497**, 781-794.

Barclay, C. J., Woledge, R. C. and Curtin, N. A. (2010). Is the efficiency of mammalian (mouse) skeletal muscle temperature dependent? *J. Physiol.* **588**, 3819-3831.

Bershitsky, S., Tsaturyan, A., Bershitskaya, O., Mashanov, G., Brown, P., Webb, M. and Ferenczi, M. A. (1996). Mechanical and structural properties underlying contraction of skeletal muscle fibers after partial 1-ethyl-3-[3-dimethylamino)propyl]carbodiimide cross-linking. *Biophys. J.* **71**, 1462-1474.

Bershitsky, SYu, and Tsaturyan, A. K. (1989). Effect of joule temperature jump on tension and stiffness of skinned rabbit muscle fibers. *Biophys. J.* **56**, 809-816.

Blough, E. R., Rennie, E. R., Zhang, F. and Reiser, P. J. (1996). Enhanced electrophoretic separation and resolution of myosin heavy chains in mammalian and avian skeletal muscles. *Anal. Biochem.* **233**, 31-35.

Bone, Q., Johnston, I. A., Pulsford, A. and Ryan, K. P. (1986). Contractile properties and ultrastructure of three types of muscle fibre in the dogfish myotome. *J. Muscle Res. Cell Motil.* **7**, 47-56.

Bottinelli, R., Schiaffino, S. and Reggiani, C. (1991). Force-velocity relations and myosin heavy chain isoform compositions of skinned fibres from rat skeletal muscle. *J. Physiol.* **437**, 655-672.

Bottinelli, R., Canepari, M., Pellegrino, M. A. and Reggiani, C. (1996). Force–velocity properties of human skeletal muscle fibres: myosin heavy chain isoform and temperature dependence. *J. Physiol.* **495**, 573-586.

Cecchi, G., Colomo, F. and Lombardi, V. (1978). Force–velocity relation in normal and nitrate-treated frog single muscle fibres during rise of tension in an isometric tetanus. *J. Physiol.* **285**, 257-273.

Claflin, D. R., Larkin, L. M., Cederna, P. S., Horowitz, J. F., Alexander, N. B., Cole, N. M., Galecki, A. T., Chen, S., Nyquist, L. V., Carlson, B. M. et al. (2011). Effects of high- and low-velocity resistance training on the contractile properties of skeletal muscle fibers from young and older humans. *J. Appl. Physiol.* **111**, 1021-1030.

Curtin, N. A. and Woledge, R. C. (1988). Power output and force-velocity relationship of live fibres from white myotomal muscle of the dogfish, *Scyliorhinus canicula*. *J. Exp. Biol.* **140**, 187-197.

Curtin, N. A., Gardner-Medwin, A. R. and Woledge, R. C. (1998). Predictions of the time course of force and power output by dogfish white muscle fibres during brief tetani. *J. Exp. Biol.* **201**, 103-114.

Curtin, N. A., Woledge, R. C. and Aerts, P. (2005). Muscle directly meets the vast power demands in agile lizards. *Proc. Biol. Sci.* **272**, 581-584.

Ducomps, C., Remignon, H., Doutreloux, J. P., Lebas, F. and Mauriege, P. (2004). Effects of prolonged jump training on fibers' distribution and fat content in rabbit skeletal muscle. *J. Exercise Physiol.* **7**, 27-36.

Edman, K. A. and Hwang, J. C. (1977). The force–velocity relationship in vertebrate muscle fibres at varied tonicity of the extracellular medium. *J. Physiol.* **269**, 255-272.

Edman, K. A., Mulieri, L. A. and Scubon-Mulieri, B. (1976). Non-hyperbolic force-velocity relationship in single muscle fibres. *Acta Physiol. Scand.* **98**, 143-156.

Ferenczi, M. A., Goldman, Y. E. and Simmons, R. M. (1984). The dependence of force and shortening velocity on substrate concentration in skinned muscle fibres from *Rana temporaria*. *J. Physiol.* **350**, 519-543.

Gilliver, S. F., Degens, H., Rittweger, J., Sargeant, A. J. and Jones, D. A. (2009). Variation in the determinants of power of chemically skinned human muscle fibres. *Exp. Physiol.* **94**, 1070-1078.

Goto, M., Kawai, M., Nakata, M., Itamoto, K., Miyata, H., Ikebe, Y., Tajima, T. and Wada, N. (2013). Distribution of muscle fibers in skeletal muscles of the cheetah (*Acinonyx jubatus*). *Mamm. Biol.* 78, 127-133.

Hamalainen, N. and Pette, D. (1993). The histochemical profiles of fast fiber types IIB, IID, and IIA in skeletal muscles of mouse, rat, and rabbit. *J. Histochem. Cytochem.* **41**, 733-743.

Hanes, M. C., Weinzweig, J., Panter, K. E., McClellan, W. T., Caterson, S. A., Buchman, S. R., Faulkner, J. A., Yu, D., Cederna, P. S. and Larkin, L. M. (2008). The effect of cleft palate repair on contractile properties of single permeabilized muscle fibers from congenitally cleft goat palates. *Ann. Plast. Surg.* **60**, 188-193.

He, Z. H., Chillingworth, R. K., Brune, M., Corrie, J. E., Trentham, D. R., Webb, M. R. and Ferenczi, M. A. (1997). ATPase kinetics on activation of rabbit and frog permeabilized isometric muscle fibres: a real time phosphate assay. *J. Physiol.* **501**, 125-148.

He, Z., Stienen, G. J., Barends, J. P. and Ferenczi, M. A. (1998). Rate of phosphate release after photoliberation of adenosine 5′-triphosphate in slow and fast skeletal muscle fibers. *Biophys. J.* **75**, 2389-2401.

He, Z. H., Chillingworth, R. K., Brune, M., Corrie, J. E., Webb, M. R. and Ferenczi, M. A. (1999). The efficiency of contraction in rabbit skeletal muscle fibres, determined from the rate of release of inorganic phosphate. *J. Physiol.* **517**, 839-854.

He, Z. H., Bottinelli, R., Pellegrino, M. A., Ferenczi, M. A. and Reggiani, C. (2000). ATP consumption and efficiency of human single muscle fibers with different myosin isoform composition. *Biophys. J.* **79**, 945-961.

Holland, P. W. and Welsch, R. E. (1977). Robust regression using iteratively reweighted least-squares. *Commun. Stat. Theory Methods* **6**, 813-827.

Hudson, P. E., Corr, S. A., Payne-Davis, R. C., Clancy, S. N., Lane, E. and Wilson, A. M. (2011). Functional anatomy of the cheetah (*Acinonyx jubatus*) hindlimb. *J. Anat.* **218**, 363-374.

Hyatt, J. P., Roy, R. R., Rugg, S. and Talmadge, R. J. (2010). Myosin heavy chain composition of tiger (*Panthera tigris*) and cheetah (*Acinonyx jubatus*) hindlimb muscles. *J. Exp. Zool. A* **313**, 45-57.

Knuth, S. T., Dave, H., Peters, J. R. and Fitts, R. H. (2006). Low cell pH depresses peak power in rat skeletal muscle fibres at both 30°C and 15°C: implications for muscle fatigue. *J. Physiol.* **575**, 887-899.

Kohn, T. A. and Noakes, T. D. (2013). Lion (*Panthera leo*) and caracal (*Caracal caracal*) type IIx single muscle fibre force and power exceed that of trained humans. *J. Exp. Biol.* **216**, 960-969.

Laemmli, U. K. (1970). Cleavage of structural proteins during the assembly of the head of bacteriophage T4. *Nature* **227**, 680-685.

Linari, M., Dobbie, I., Reconditi, M., Koubassova, N., Irving, M., Piazzesi, G. and Lombardi, V. (1998). The stiffness of skeletal muscle in isometric contraction and rigor: the fraction of myosin heads bound to actin. *Biophys. J.* **74**, 2459-2473.

Mellors, L. J. and Barclay, C. J. (2001). The energetics of rat papillary muscles undergoing realistic strain patterns. *J. Exp. Biol.* **204**, 3765-3777.

Morrissey, J. H. (1981). Silver stain for proteins in polyacrylamide gels: a modified procedure with enhanced uniform sensitivity. *Anal. Biochem.* **117**, 307-310.

Picquet, F. and Falempin, M. (2003). Compared effects of hindlimb unloading versus terrestrial deafferentation on muscular properties of the rat soleus. *Exp. Neurol.* **182**, 186-194.

Ranatunga, K. W. (1982). Temperature-dependence of shortening velocity and rate of isometric tension development in rat skeletal muscle. *J. Physiol.* **329**, 465-483.

Ranatunga, K. W. (1984). The force–velocity relation of rat fast- and slow-twitch muscles examined at different temperatures. *J. Physiol.* **351**, 517-529.

Ranatunga, K. W. (1998). Temperature dependence of mechanical power output in mammalian (rat) skeletal muscle. *Exp. Physiol.* **83**, 371-376.

Ranatunga, K. W. (2010). Force and power generating mechanism(s) in active muscle as revealed from temperature perturbation studies. *J. Physiol.* **588**, 3657-3670.

Rome, L. C., Sosnicki, A. A. and Goble, D. O. (1990). Maximum velocity of shortening of three fibre types from horse soleus muscle: implications for scaling with body size. *J. Physiol.* **431**, 173-185.

Seow, C. Y. and Ford, L. E. (1991). Shortening velocity and power output of skinned muscle fibers from mammals having a 25,000-fold range of body mass. *J. Gen. Physiol.* **97**, 541-560.

Sharp, N. C. C. (1997). Timed running speed of the cheetah (*Acinonyx jubatus*). *J. Zool.* **241**, 493-494.

Sonnenblick, E. H. (1964). Series elastic and contractile elements in heart muscle: changes in muscle length. *Am. J. Physiol.* **207**, 1330-1338.
Spence, A. J., Thurman, A. S., Maher, M. J. and Wilson, A. M. (2012). Speed, pacing strategy and aerodynamic drafting in thoroughbred horse racing. *Biol. Lett.* **8**, 678-681.
Sun, Y. B., Hilber, K. and Irving, M. (2001). Effect of active shortening on the rate of ATP utilisation by rabbit psoas muscle fibres. *J. Physiol.* **531**, 781-791.
Thirlwell, H., Corrie, J. E., Reid, G. P., Trentham, D. R. and Ferenczi, M. A. (1994). Kinetics of relaxation from rigor of permeabilized fast-twitch skeletal fibers from the rabbit using a novel caged ATP and apyrase. *Biophys. J.* **67**, 2436-2447.
Usherwood, J. R. and Wilson, A. M. (2005). Biomechanics: no force limit on greyhound sprint speed. *Nature* **438**, 753-754.
Widrick, J. J., Trappe, S. W., Costill, D. L. and Fitts, R. H. (1996). Force–velocity and force–power properties of single muscle fibers from elite master runners and sedentary men. *Am. J. Physiol. Cell Physiol.* **271**, C676-C683.
Williams, T. M., Dobson, G. P., Mathieu-Costello, O., Morsbach, D., Worley, M. B. and Phillips, J. A. (1997). Skeletal muscle histology and biochemistry of an elite sprinter, the African cheetah. *J. Comp. Physiol. B* **167**, 527-535.
Wilson, A. M., Lowe, J. C., Roskilly, K., Hudson, P. E., Golabek, K. A. and McNutt, J. W. (2013). Locomotion dynamics of hunting in wild cheetahs. *Nature* **498**, 185-189.